Disulfide Formation and Stability of a Cysteine-Rich Repeat Protein from *Helicobacter pylori*†

V. Sathya Devi, Christine Berger Sprecher, Peter Hunziker, Peer R. E. Mittl, Hans Rudolf Bosshard,* and Ilian Jelesarov

Biochemisches Institut der Universität Zürich, Winterthurerstrasse 190, CH-8057 Zürich, Switzerland

Received November 17, 2005; Revised Manuscript Received December 20, 2005

ABSTRACT: *Helicobacter pylori* cysteine-rich proteins (Hcps) are disulfide-containing repeat proteins. The repeating unit is a 36-residue, disulfide-bridged, helix-loop-helix motif. We use the protein HcpB, which has four repeats and four disulfide bridges arrayed in tandem, as a model to determine the thermodynamic stability of a disulfide-rich repeat protein and to study the formation and the contribution to stability of the disulfide bonds. When the disulfide bonds are intact, the chemical unfolding of HcpB at pH 5 is cooperative and can be described by a two-state reaction. Thermal unfolding is reversible between pH 2 and 5 and irreversible at higher pH 5. Differential scanning calorimetry shows noncooperative structural changes preceding the main thermal unfolding transition. Unfolding of the oxidized protein is not an all-or-none two-state process, and the disulfide bonds prevent complete unfolding of the polypeptide chain. The reduced protein is significantly less stable and does not unfold in a cooperative way. During oxidative refolding of the fully reduced protein, all the possible disulfide intermediates with a correct disulfide bond are formed. Formation of "wrong" (non-native) disulfide bonds could not be demonstrated, indicating that the reduced protein already has some partial repeating structure. There is a major folding intermediate with disulfides in the second, third, and fourth repeat and reduced cysteines in the first repeat. Disulfide formation in the first repeat limits the overall rate of oxidative refolding and contributes about half of the thermodynamic stability to native HcpB, estimated as 27 kJ mol^{-1} at 25 °C and pH 7. The high contribution to stability of the first repeat may be explained by the repeat acting as a cap to protect the hydrophobic interior of the molecule.

Repeat proteins are built of structurally identical motifs arranged in tandem to form elongated shapes. The proteins have nonglobular structures and form specific binding surfaces functioning as versatile scaffolds for protein−protein interactions in signaling and regulatory pathways (*1*−*5*) (for a classification of repeat proteins see http://cmm.info.nih.gov/kajava/solenoidtable.html). Repeat proteins designed by protein engineering have great potential as binding partners (*6*, *7*). The repeating motifs typically have 20−40 residues forming secondary structures that coalesce in various topologies (*3*). The linear stacking of repeat modules produces local, short-range packing interactions at the inter-repeat interface. Long-range interactions between sequentially distant residues are rare. The stability of a repeat protein may be dissected into the intrinsic free energy of the individual repeats and the coupling free energies between the repeats (*8*). Thus, folding pathways may be predicted to be heterogeneous, passing through multiple states and exhibiting heterogeneity. However, there are yet few experimental studies on the folding of repeat proteins (*2*, *9*, *10*).

A family of cysteine-rich repeat proteins has been detected as open reading frames in the genome of *Helicobacter pylori* (*11*, *12*). Gram-negative *H. pylori* is responsible for several gastric and duodenal diseases (*13*, *14*). The precise biological function of Hcps[1] is not known. Some Hcps bind β-lactam compounds (*12*, 15) and may be involved in the innate immune response (*16*). The proteins are built of several consecutive, 36-residues-long α/α motifs, the antiparallel α-helices of the motifs being connected by a short loop. The structure belongs to the Sel1-like protein family, a subfamily of the tetratricopeptide repeat proteins (*5*). The α-helices of each repeat are bridged by a disulfide bond. Although cysteines are found in other repeat proteins, disulfide bonds are a specific feature of Hcps. Disulfide bonds have been reported only in one structurally unrelated antifreeze repeat protein (*17*).

† This work was supported in part by the Swiss National Science Foundation and by NCCR Structural Biology.

* Address correspondence to Hans Rudolf Bosshard, Biochemisches Institut der Universität Zürich, Winterthurerstrasse 190, CH-8057 Zürich, Switzerland. Telephone: +41 44 929 1029. Fax: +41 44 635 6805. E-mail: h.r.bosshard@bioc.unizh.ch.

[1] Abbreviations: CD, circular dichroism; CDAP, 1-cyano-4-(dimethylamino)-pyridiniumtetrafluoroborate; DSC, differential scanning calorimetry; DTT, dithiothreitol; ESI-MS, electrospray ionization mass spectrometry; GdmCl, guanidinium chloride; GSH and GSSG, reduced and oxidized glutathione, respectively; Hcps, *Helicobacter pylori* cysteine-rich proteins; HcpB, HP0336 gene product of the Hcp family; $HcpB_{234}$, major folding intermediate with disulfide bonds in the second, third, and fourth repeat, respectively; $HcpB_{\Delta}1$, truncated HcpB lacking the first repeat motif; MALDI-TOF, matrix-assisted laser desorption/ionization-time-of-flight mass spectrometry; MRE, mean ellipticity per mole of amino acid residue; Ni−NTA, nickel−nitrilotriacetic acid; RP-HPLC, reversed-phase high-performance liquid chromatography; TFA, trifluoroacetic acid.

10.1021/bi052352u CCC: $33.50
Published on Web 01/20/2006

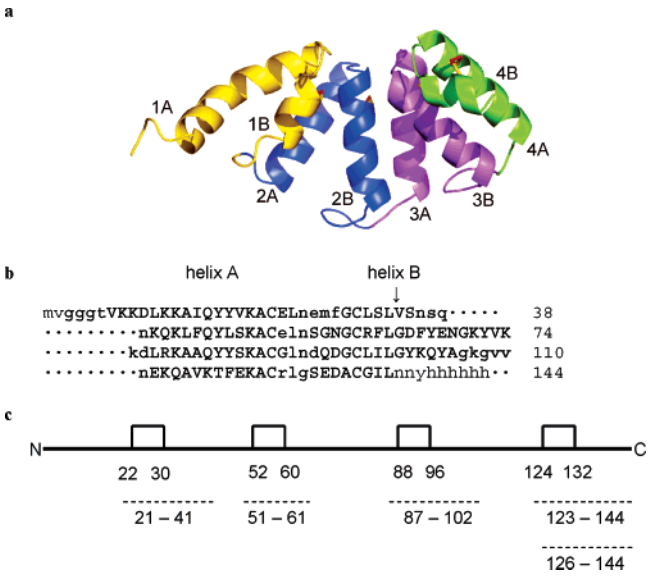

FIGURE 1: Structure of HcpB. (a) Crystal structure of HcpB. The four repeat motifs have different colors; disulfide bridges are shown in red. Note that the assignment of helices A and B to repeats 1−4 follows the definition of Luthy et al. (*18*), which differs from the assignment used for tetratricopeptide repeats (*5*). (b) Sequence of HcpB with C-terminal His-tag. The four repeats are colored as in panel a and aligned for sequence homology. Residues in lower case are not part of helices; black residues are not seen in the 3D structure shown in panel a. The arrow indicates cleavage after Ser-32 by thermolysine, producing the truncated derivative $HcpB_{\Delta}1$ corresponding to residues 33−144. (c) Pattern of sequential disulfide bonds (boxes with position of cysteines indicated) and of the cysteine-containing tryptic peptides (dashed lines). Numbers indicate the N- and C-terminal residues of the peptides. Peptide 126−144 is produced only if Cys124 is reduced, peptide 123−144 only if disulfide Cys124−Cys132 is present.

In a first attempt to study the role and importance of the disulfide bonds of Hcps, we have chosen HcpB as a model, since it is the shortest Hcp family member with only four repeat units and four disulfides bridges (Figure 1) (*18*). We have tried to answer two questions: What is the contribution of the disulfide bonds to the stability of HcpB and how are disulfide bonds formed during oxidative refolding of the fully reduced polypeptide chain? One may envisage two extreme cases for disulfide formation. If fully reduced HcpB is a random coil lacking repeat-like structure, formation of wrong, that is, of non-native disulfide bonds during oxidative refolding would be likely. Wrong disulfide bonds formed transitorily during folding have to be reshuffled to the native connectivity. Reshuffling is typical for the oxidative refolding of globular disulfide proteins, both in vitro and in the cell where special enzyme systems accomplish disulfide exchange (*19*, *20*). If, on the other hand, repeat-like features appear before disulfide formation, incorrect disulfide bonds should have a small chance of building up during oxidative refolding of HcpB. Indeed, non-native disulfide bonds could not be found in oxidative refolding of HcpB. The folding reaction is characterized by the consecutive appearance of intermediates with one, two, and three correct disulfide bonds, of which one three-disulfide intermediate is a major folding intermediate whose transition to the native protein is rate-limiting.

MATERIALS AND METHODS

Buffers and Chemicals. Standard buffer was 20 mM sodium phosphate and 100 mM KCl, pH 7.0. Redox buffer consisted of standard buffer containing 2 mM GSH and 1 mM GSSG. Universal buffer was 7.5 mM each of boric, citric, and phosphoric acid adjusted to the desired pH with KOH and to an ionic strength of 100 mM with KCl. Chemicals were of analytical grade or of the best grade available and were used without further purification.

Expression and Purification of HcpB. Recombinant HcpB, C-terminally extended by a 6-His tag (Figure 1b), was expressed in *Escherichia coli*, solubilized from inclusion bodies, and affinity-purified on Ni−NTA agarose as described (*18*). The protein was desalted and freeze-dried, and the mass of 16 160.5 Da (including the 6-His tag) was confirmed by mass spectrometry. The protein concentration was determined by UV spectroscopy using $\epsilon_{276} = 15\,080$ cm^{-1} M^{-1}. Reduced HcpB was prepared by overnight incubation of the protein (0.4 mg mL^{-1}) at room temperature in a sealed vial with 15 mM DTT in universal buffer of pH 7. The pH was adjusted as necessary, and the material was kept under argon. Complete reduction of the four disulfide bonds was confirmed by mass analysis after reaction of the free sulfhydryl groups with CDAP (see Trapping of Intermediates by Cyanylation).

CD Spectroscopy. Experiments were performed on a J-715 spectropolarimeter (Jasco) equipped with a temperature-controlled water bath, using cylindrical jacketed cuvettes of 1 mm optical path length. Spectra were recorded three times between 200 and 250 nm at a scanning rate of 5 nm min^{-1}. Thermal melting curves were recorded by continuous heating at 1 °C min^{-1}, and the ellipticity at 222 nm was collected every 10 s. Reversibility was determined from the recovery of the ellipticity after cooling. Thermal melting curves were analyzed as described before (*10*).

For measuring unfolding by urea, CD spectra were taken after overnight incubation of the protein at the desired urea concentration. In the case of the major intermediate $HcpB_{234}$, cysteine oxidation was prevented by keeping all solutions saturated with argon. The integrity of $HcpB_{234}$ after urea unfolding was confirmed by RP-HPLC and ESI-MS. Assuming a two-state folding reaction, the signal change at 222 nm was analyzed according to $[\theta] = (K_U/(1 - K_U))([\theta_U] - [\theta_F]) + [\theta_F]$, where K_U is the unfolding constant defined as $f_U/(1 - f_U)$ and f_U is the fraction of unfolded protein. $[\theta]$ is the molar ellipticity per residue at 222 nm, and $[\theta_F]$ and $[\theta_U]$ are the molar ellipticity per residue of folded and unfolded protein, respectively, assumed to be linear functions of [urea] of the form $[\theta_i] = [\theta_{i,0}] + \alpha_i$[urea]. The free energy of unfolding in the absence of urea, ΔG_U^W, was extrapolated from $\Delta G_U = \Delta G_U^W - m$[urea], where $\Delta G_U = -RT \ln K_U$.

Differential Scanning Calorimetry. The temperature dependence of the heat capacity of HcpB (disulfides intact) was determined with a VP-DSC calorimeter (MicroCal LLC, Northampton, MA) at a heating rate of 1 °C min^{-1}. Details on the performance of the instrument are given elsewhere (*21*). After subtraction of the buffer versus buffer baseline, the data were transformed to partial specific heat capacity using a partial specific volume of 0.718 cm^{-3} g^{-1} calculated from the amino acid sequence (*22*). The data were analyzed by nonlinear least-squares regression using the program CpCalc 2.1 (Applied Thermodynamics) or in-house scripts written for NLREG (Phillip Sherod) utilizing thermodynamic modeling as described previously (*23*).

Oxidative Refolding. HPLC-purified, recombinant HcpB (1 mg mL^{-1}) was treated with 5 M GdmCl and 0.1 M DTT in standard buffer for 2 h at room temperature. GdmCl and DTT were rapidly removed by passing the reaction mixture through a Hi-trap desalting column (Sephadex G-25, Amersham Biosciences), which had been preequilibrated in standard buffer. The eluate was captured in freshly prepared redox buffer to start oxidative refolding. The final concentration of HcpB in the redox buffer was 0.5 mg mL^{-1}. Samples were removed at timed intervals, and cysteine oxidation was quenched by adding an equal volume of 8% TFA. Samples were chromatographed by RP-HPLC on a Vydac C8 analytical column (4.6 mm × 250 mm, Nucleosil 300-5). The column was eluted with a linear gradient from 46% to 54% solvent B in solvent A at a flow rate of 0.7 mL min^{-1}. Solvent A was 3% acetonitrile and 0.1% TFA in water; solvent B was 80% acetonitrile and 0.085% TFA in water. Peaks were collected, lyophilized, and stored at −20 °C for further analysis.

Trapping of Intermediates by Cyanylation. Lyophilized fractions from HPLC separation were dissolved at a concentration of 0.5 mg mL^{-1} in 100 mM sodium citrate buffer, pH 3.0, and cyanylated with 0.2 M freshly prepared CDAP for 30 min at room temperature. CDAP was present in at least 20-fold molar excess over free cysteines. Cyanylated material was immediately rechromatographed by RP-HPLC to remove the reagent and to repurify the cyanylated protein fractions. Cyanylation did not markedly change the retention time in RP-HPLC. Cyanylated HcpB was digested with trypsin (trypsin/HcpB ratio 1:100) in 20 mM Tris-HCl and 50 mM NaCl, pH 7.5, for 16 h at room temperature. The digestion mixture was mass-analyzed by MALDI-TOF.

Major Intermediate $HcpB_{234}$ and Truncated $HcpB_{\Delta}1$. $HcpB_{234}$ produced during oxidative refolding was purified by RP-HPLC and kept in argon-saturated standard buffer for use in CD spectroscopy and urea unfolding studies. Its concentration was determined from $\epsilon_{276} = 15\,080\ cm^{-1}\ M^{-1}$. Derivative $HcpB_{\Delta}1$ lacking repeat 1 was prepared by limited proteolysis with thermolysine. HcpB (1 mg) was incubated with thermolysine (Sigma, P-1512) in 1 mL of 50 mM *N*-ethylmorpholine-acetate buffer, pH 6.4 (thermolysine/protein ratio 1:100) at 30 °C for 1 h. The digestion mixture was separated by RP-HPLC; peaks were collected, analyzed by MALDI-TOF, and subjected to automated Edman degradation. The concentration of $HcpB_{\Delta}1$ was calculated from $\epsilon_{276} = 12\,035\ cm^{-1}\ M^{-1}$.

Mass Analysis. ESI-MS was performed on a QTOF Ultima API (Waters) instrument in 0.2% formic acid and 50% acetonitrile at a flow rate of 0.8 μL min^{-1}. MALDI-TOF analysis was performed on a Biflex III (Bruker) instrument using the α-cyano-4-hydroxy cinnamic acid matrix.

RESULTS AND DISCUSSION

We first describe the thermal and chemical unfolding of native and fully reduced HcpB to assess the overall stability contribution of the four disulfide bonds.

Thermal Stability of HcpB Followed by CD. Temperature-induced unfolding curves for native HcpB were followed by CD at 222 nm (Figure 2). Unfolding is cooperative and can be approximated by a two-state unfolding reaction. The stability decreases with decreasing pH. The midpoint temperature of unfolding, T_m, decreases from 64.8 °C at pH 5 to 39.3 °C at pH 2. Thermal unfolding is at least 85% reversible at pH 5 and below yet becomes irreversible above pH 5. Below 10 °C and above 70 °C, the traces of the mean residue ellipticity are very similar from pH 2 to 5, indicating that the helical content of the native state and the structure of the denatured state are not appreciably altered by pH. In contrast to HcpB with intact disulfide bonds, the fully reduced molecule does not unfold cooperatively. MRE_{222} increases continuously between 0 and 80 °C with only a faint change of slope around 60 °C (thin line in Figure 2). The gradual increase of MRE_{222} with temperature indicates that the reduced protein has some residual secondary structure.

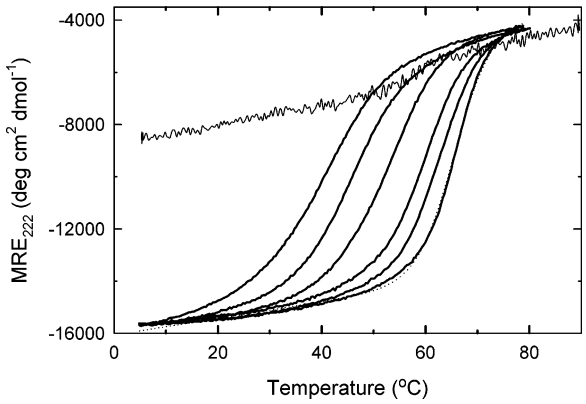

FIGURE 2: Thermal melting of oxidized HcpB (disulfides intact) observed by CD spectroscopy. The change of the mean residue ellipticity at 222 nm with temperature upon continuous heating (1 °C min^{-1}) is shown at pHs 2, 2.4, 3, 3.5, 4, and 5 (left to right). The melting curves can be approximated by a two-state folding reaction; a best fit for the curve at pH 5 is shown as a dotted line. Melting of fully reduced HcpB in the presence of 15 mM DTT at pH 5 spans only a small change of ellipticity and is noncooperative (thin line). Experiments were performed in universal buffer adjusted to the desired pH.

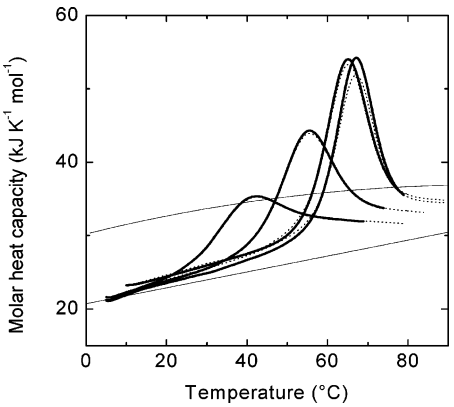

FIGURE 3: Thermal melting of oxidized HcpB (disulfide bonds intact) observed by DSC. The change of the molar heat capacity of HcpB (150 μM) upon continuous heating at 1 °C min^{-1} is shown at pHs 2, 3, 4, and 5 (left to right). Dotted lines are repeat heating curves to demonstrate reversibility. The upper thin line is the calculated heat capacity for the completely unfolded protein (*25*); the lower thin line is the calculated heat capacity of a globular protein of the size of HcpB (*24*).

Thermal Stability of HcpB Followed by DSC. Thermal melting was followed also by DSC. Figure 3 shows the DSC traces for the melting of HcpB at pHs 2, 3, 4, and 5. The partial specific heat capacity at 25 °C is close to the values measured for typical globular proteins but exhibits a steeper increase with temperature from $8.5 \times 10^{-3}\ J\ g^{-1}\ K^{-2}$ at pH

Table 1: Thermodynamic Parameters Describing the Thermal Melting of HcpB as Followed by DSC and CD Spectroscopy[a]

pH	T_m (°C) CD	ΔH_m^{vH} (kJ/mol) CD	T_m (°C) DSC	ΔH_m^{vH} (kJ/mol) DSC	ΔH_m^{cal} (kJ/mol) DSC
2	39.3	122	40.4	182	130
2.4	45.2	145			
3	51.7	157	53.3	216	225
3.5	58.7	193			
4	61.6	210	64.4	283	287
5	64.8	270	66.3	304	280

[a] Calculated maximum errors: ΔH_m^{vH}, 12%; ΔH_m^{cal}, 8%; T_m, 0.3 °C.

5 to 13.8 × 10^{-3} J g^{-1} K^{-2} at pH 2 as compared to the reference value of (6.7 ± 1) × 10^{-3} J g^{-1} K^{-2} for globular proteins (*24*). The transitions are relatively broad, especially at low pH. The heat capacity of the denatured state is lower than the predicted heat capacity of a fully solvated polypeptide chain with the amino acid composition of HcpB (*25*). The two-state model of cooperative unfolding does not describe the measured melting traces well. The minimal model that fits reasonably well with the experiment includes an intermediate that is populated at temperatures preceding the main heat absorption peak. In view of the poor statistical significance of the modeling (highly coupled T_m and ΔH_m describing the transition from the native state to the state preceding the main unfolding event), it appears likely that the low-temperature, premelting transition is noncooperative and involves sequentially interconverting intermediates. In accordance with statistical-mechanical modeling, the native state undergoes a transition to the putative intermediate(s) that is accompanied by a low enthalpy change (~10−20% of the enthalpy of the main transition) yet by a significant heat capacity increment (as high as ΔC_p of the main transition). The per-residue unfolding enthalpy (2.1 kJ (mol res)$^{-1}$), unfolding entropy (6.3 J K^{-1} (mol res)$^{-1}$), and unfolding heat capacity change (25−30 J K^{-1} (mol res)$^{-1}$) calculated at 65 °C are among the lowest values measured for proteins (*26*). We conclude that at the on-set of the main unfolding event HcpB is quite flexible and less well-packed than at lower temperatures. Unfolding proceeds to a denatured state which is conformationally constrained, may contain residual tertiary contacts, and is not completely hydrated.

Table 1 lists the unfolding enthalpies calculated from CD and DSC experiments. In accordance with the DSC data, the main unfolding transition of HcpB is rather cooperative between pH 3 and 5, as judged by the ratio between the model-independent calorimetric and the model-dependent van't Hoff enthalpies, $\Delta H_m^{vH,DSC}/\Delta H_m^{cal}$, which is close to unity. At pH 2, $\Delta H_m^{vH,DSC}/\Delta H_m^{cal}$ is 1.3. Since melting is perfectly reversible at pH 2 and the protein is monomeric, the reason for the higher enthalpy ratio is not clear. However, the van't Hoff enthalpies from CD experiments are systematically lower than the van't Hoff enthalpies calculated from DSC data. Furthermore, the fraction of unfolded protein, f_U, changes in a nonparallel fashion with temperature when calculated from CD or DSC data (Table 1). The temperature of half-unfolding (f_U = 0.5) is systematically higher in the DSC experiment, especially below pH 5. It is likely, therefore, that melting of the secondary structure monitored by CD precedes the disruption of gross-packing interactions revealed by DSC.

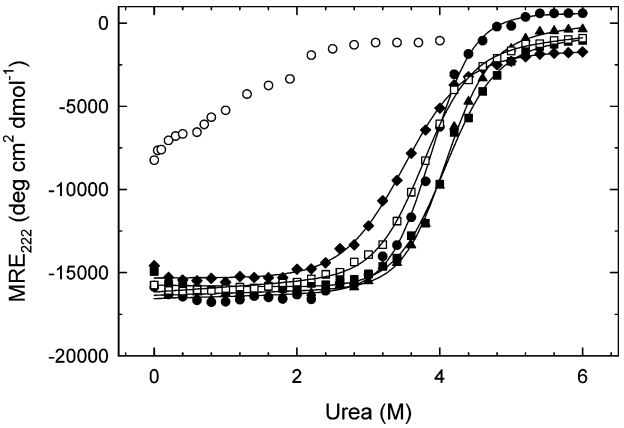

FIGURE 4: Unfolding of HcpB by urea. The change of the mean residue ellipticity at 222 nm of oxidized HcpB (disulfides intact) was measured at increasing urea concentration at pH 5 and 5 °C (circles), 15 °C (triangles), 25 °C (squares), 40 °C (diamonds), and at pH 7 and 25 °C (open squares). Unfolding of fully reduced HcpB in the presence of 15 mM DTT at 5 °C and pH 5 is noncooperative (open circles). Solid lines are best fits for two-state unfolding of oxidized HcpB. Experiments were performed in universal buffer adjusted to pH 5 at the desired temperature and in standard buffer at pH 7.

Stability of HcpB Followed by Unfolding with Urea. Chemical unfolding with urea was performed at pH 7 and 25 °C and in the temperature range of 5−40 °C at pH 5.0 (Figure 4). Transitions are reversible. Interestingly, the ellipticity decreases at high urea concentration and increasing temperature, indicating temperature-induced structural variation of the urea-denatured state. Another peculiarity is the small but reproducible decrease of MRE_{222} between 0 and 0.5 M urea. This effect is possibly caused by small structural rearrangements due to protein−urea interactions. As in thermal unfolding (Figure 2), the fully reduced HcpB unfolds in a noncooperative manner when treated with urea. In accord with the thermal unfolding data, the reduced protein seems to lack a well-defined and compact structure that would give rise to cooperative unfolding. Nevertheless, the increase of the CD signal from 0 to 4 M urea indicates that the reduced protein keeps a certain amount of secondary structure. This is also supported by the CD spectra shown in Figure 5. The helix content of fully reduced HcpB calculated from the value of MRE_{220} (*27*) is about 50% of that of the native protein.

With the help of the thermal and chemical unfolding data, the stability curve of HcpB at pH 5 could be constructed using the Gibbs−Helmholtz equation

$$\Delta G(T) = \Delta H_m\left(1 - \frac{T}{T_m}\right) + \Delta C_p\left(T - T_m - T\ln\frac{T}{T_m}\right) \quad (1)$$

ΔH_m is the unfolding enthalpy at the reference temperature T_m, where the fractional populations of folded and unfolded protein are equal (f_u = 0.5), and ΔC_p is the heat capacity increment. The curve calculated according to eq 1 is shown in Figure 6. Regression analysis using the four ΔG values obtained from chemical unfolding between 5 and 40 °C combined with ΔG = 0 at the thermal melting temperature yields ΔH_m = 370 ± 50 kJ mol^{-1}. This value exceeds by far the value of ΔH_m obtained from direct thermal unfolding experiments (270−300 kJ mol^{-1}). The calculated ΔC_p is 6.1

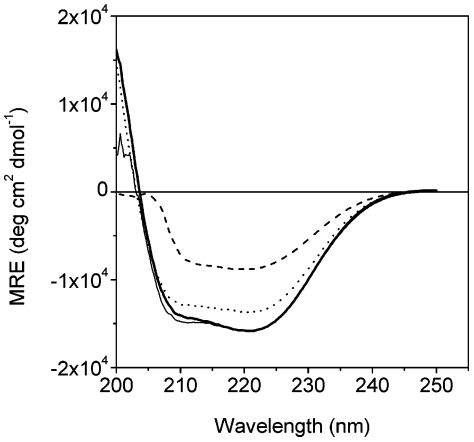

FIGURE 5: CD spectra of HcpB and its derivatives. Native HcpB (disulfides intact, thick solid line), reduced HcpB in the presence of 15 mM DTT (dashed line), $HcpB_{\Delta}1$ lacking the first repeat motif (thin line), and major folding intermediate $HcpB_{234}$ (dotted line). Spectra were measured in standard buffer at pH 7 and 20 °C.

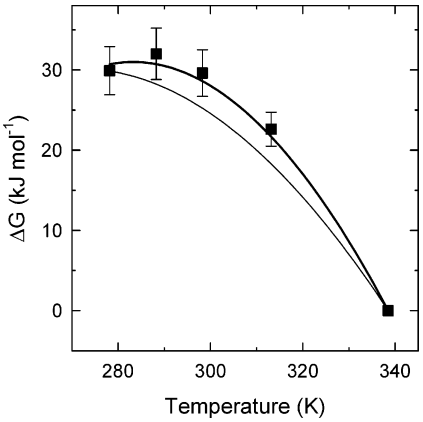

FIGURE 6: Stability curve at pH 5 of oxidized HcpB (disulfides intact). The four data points between 5 and 40 °C are ΔG-values obtained from urea unfolding experiments. The right-most data point corresponds to $\Delta G = 0$ from thermal unfolding. The thick line is a best fit using the Gibbs−Helmholtz eq 1 with $\Delta H_m = 370 \pm 50$ kJ mol^{-1}, $\Delta C_p = 6.1 \pm 1.7$ kJ K^{-1} mol^{-1}, and $T_m = 65.3 \pm 0.1$ °C. The ΔG-function shown as a thin line was calculated with $\Delta H_m = 295$ kJ mol^{-1} and $\Delta C_p = 4.0$ kJ K^{-1} mol^{-1} measured by DSC. See the text for a detailed discussion.

$\pm$ 1.7 kJ K^{-1}mol^{-1}, which is also larger than the calorimetric value of 4.0 $\pm$ 0.3 kJ K^{-1} mol^{-1} yet is of similar magnitude as ΔC_p of 5.5−7.5 kJ K^{-1} mol^{-1} calculated from Kirchoff's plots using the three different sets of ΔH_m listed in Table 1. The thin line in Figure 5 represents the stability curve calculated with ΔH_m and ΔC_p from DSC. When compared to thermal unfolding, urea-induced unfolding predicts a slightly higher stability at benign temperature and a higher temperature of maximum stability. Two explanations are likely. The unfolding mechanism differs depending on whether heat or urea is used as the denaturing agent. Alternatively, the native state and/or the denatured state vary in terms of structure and energetic content and are thermodynamically different in plain buffer and urea-containing solution (*28*). Overall, the observed inconsistency of stability, enthalpy, and heat capacity estimates together with the discrepancies between ΔH_m and T_m from spectroscopy and calorimetry, and the presence of gradual, noncooperative, temperature-induced structural changes strongly suggest that unfolding of HcpB with its disulfide bonds intact proceeds through several steps.

Disulfide Formation. We now describe the oxidative refolding of reduced HcpB in the presence of the GSH/GSSG redox pair. Already in Anfinsen's seminal paper of 1961, it was conjectured that oxidative refolding of a disulfide-containing protein is a dynamic process involving rapid closing and opening of disulfide bonds to reach the correct pairings by "trial and error" (*29*). Subsequent work on ribonuclease, bovine pancreatic trypsin inhibitor, lysozyme, and many other disulfide-containing globular proteins amply demonstrated the dynamic nature of disulfide bond formation and the temporary rise and fall of incorrect disulfides (recent review in ref *30*). Hence, efficient oxidative refolding in the test tube needs a redox buffer to speed up disulfide formation and enable disulfide reshuffling if necessary. Some folding pathways depend on reaction conditions, and occasionally even on how the folding intermediates are being trapped (*30*). One feature is rather common: formation of the last disulfide bond often is rate-limiting, the conformation of the rate-limiting intermediate being close to the native state (*30*).

Disulfide formation is detected experimentally by rapidly and irreversibly blocking and identifying the remaining free thiol groups at different time points after the start of the folding reaction. Acidification is another means of quenching disulfide bond formation since disulfide formation occurs through the deprotonated thiol group. We have combined acidification and chemical blocking of free thiol groups to follow the in vitro folding pathway of HcpB.

Oxidative Refolding of HcpB Follows a Pathway with a Dominant Three-Disulfide Intermediate. Summarized briefly, the procedure to follow the oxidative refolding of HcpB was as follows. Fully reduced and chemically denatured HcpB was rapidly transferred into redox buffer at pH 7.0. Refolding was allowed to proceed at ambient temperature. Samples were taken at timed intervals, disulfide formation was quenched with TFA, and samples were analyzed by RP-HPLC under acidic conditions to prevent further oxidation. Chromatographic peaks were collected, and free sulfhydryl groups were blocked by cyanylation with 1-cyano-4-(dimethylamino)-pyridiniumtetrafluoroborate (CDAP) at pH 3 (*31*). Finally, the cyanylated products were digested with trypsin and the digestion products identified by MALDI-TOF mass spectrometry.

Oxidative refolding of HcpB had to be performed at pH 7 because disulfide formation is too slow at pH 5 where the thermodynamic properties of HcpB were determined. The refolding reaction was started by a rapid (~15 s) buffer change from reducing and denaturing conditions (100 mM DTT, 5 M GdmCl) to refolding conditions (redox buffer containing GSH and GSSG). Folding started immediately as indicated by the rapid drop of the CD signal at 222 nm. About half of the MRE_{222}-value of native HcpB was reached before 30 s, the shortest time point of manual mixing (not shown), while the oxidized protein took considerably longer to appear. Figure 7 shows the time course of disappearance of reduced HcpB and appearance of oxidized HcpB. Table 2 shows the mass analysis of the chromatographic peaks of Figure 7. Reduced protein (R) dominates during the first few minutes. Thereafter, the minor intermediates labeled as chromatographic peaks 1, 2, and 3 appear; they disappear during maximal production of the major intermediate $HcpB_{234}$.

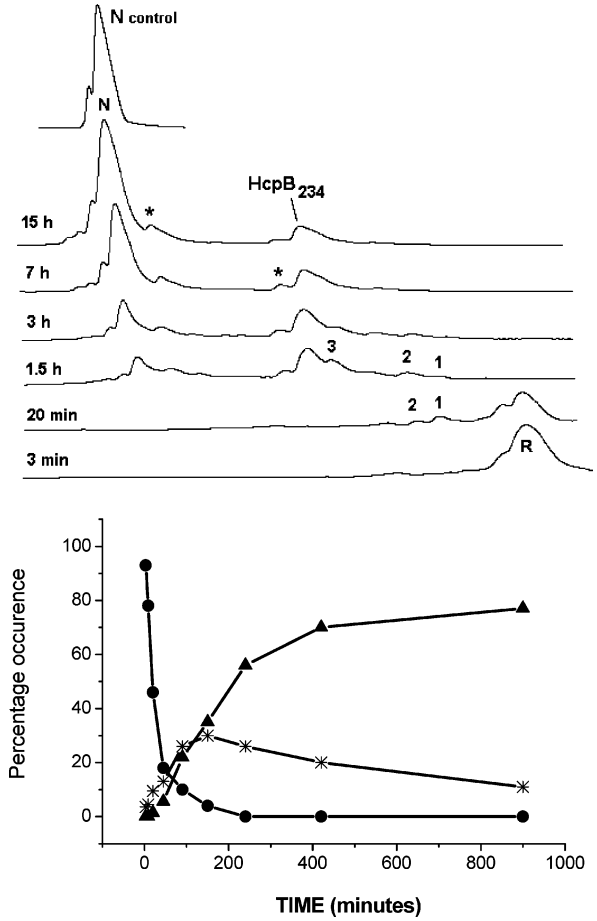

FIGURE 7: Oxidative refolding of fully reduced HcpB in redox buffer at pH 7.0 and room temperature. Top panel: chromatographic separation of reaction products by RP-HPLC after different times of refolding. R and N are the fully reduced and fully oxidized proteins, respectively. Peaks labeled 1, 2, and 3 contain folding intermediates with 1, 2, and 3 correct disulfide bonds, respectively. $HcpB_{234}$ is the major folding intermediate with disulfide bonds in the second, third, and fourth repeat. $N_{control}$ is recombinant HcpB chromatographed on the same column. The shoulder preceding R is an artifact and contains material identical to R. Material in peaks indicated by * could not be identified unequivocally (see the text). Bottom panel: time course of disappearance of reduced protein R (●) and appearance of the major intermediate $HcpB_{234}$ (*) and of the oxidized protein N (▲).

Table 2: Mass (Da) of Reaction Products of Oxidative Refolding Separated by RP-HPLC

peak in Figure 7	mass[a] (calculated)	cyanylated thiol groups/disulfides
R	16368.2 (16368.6)	8/0
peak 1	16316.3 (16316.6)	6/1
peak 2	16264.3 (16264.6)	4/2
peak 3	16212.0 (16212.5)	2/3
$HcpB_{234}$	16212.0 (16212.5)	2/3
N	16160.5 (16160.5)	0/4

[a] Average masses calculated by the program MaxEnt1 (Micromass, U.K.). The mass difference between a disulfide (cystine) and two cyanylated cysteines is 52.

Oxidized protein (N) appears after about 1 h. Mass analysis shows that the material represented by chromatographic peaks 1 and 2 contain one and two disulfide bonds, respectively, whereas the compounds represented by peak 3 and $HcpB_{234}$ both contain 3 disulfide bonds (see Table 2).

Table 3: Mass[a] (Da) of Cysteine-Containing Peptides Obtained by Tryptic Digestion of Labeled Peaks in the RP-HPLC Profile of Oxidative Refolding (Figure 7)

peptide [cyteines] (calculated mass)	N[b]	R[b]	peaks 1, 2, 3[b,c]	$HcpB_{234}$[b]
21−41 [C^{22}, C^{30}] (2298.1)	2297.9 (0)	2349.8 (2)	2297.6 (0) 2349.7 (2)	2349.8 (2)
51−61 [C^{52}, C^{60}] (1121.5)	1121.5 (0)	1173.4 (2)	1121.2 (0) 1172.3 (2)	1121.4 (0)
87−102 [C^{88}, C^{96}] (1680.8)	1680.8 (0)	1732.7 (2)	1680.5 (0) 1732.5 (2)	1680.6 (0)
123−144 [C^{124}, C^{132}] (2537.1)	2537.0 (0)		2536.7 (0)	2536.7 (0)
126−144[d] [C^{132}] (2191.0)		2215.8 (1)	2215.6 (1)	

[a] Monoisotopic masses of singly charged peptides, i.e., $[M + H]^+$; the mass difference between a disulfide (cystine) and two cyanylated cysteines is 52. [b] Number of cyanylated thiol groups in parentheses. [c] Experimental masses for peptides from peak 1; masses were the same within error for peptides from peaks 2 and 3. [d] The C-terminal fourth repeat yielded two cysteine-containing tryptic peptides; peptide 123−144 was produced only when the disulfide Cys^{124}−Cys^{132} was intact and peptides 123−125 and 126−144 only when the disulfide was reduced; peptide 123−125 was not determined.

To identify the location of the disulfide bonds in the different intermediates, the labeled chromatographic peaks of Figure 7 were cyanylated and digested with trypsin. Tryptic peptides with cysteine residues (Figure 1, panel c) were identified by MALDI-TOF mass spectrometry. The results are summarized in Table 3. Peak N represents only peptides with disulfide bonds intact, that is, no cyanylated thiol groups. Peak R represents all the cyanylated peptides, that is, those without disulfides. Digestion of the material represented by peaks 1, 2, and 3 yields mixtures of all the cyanylated and noncyanylated tryptic peptides. This means that in the early phase of oxidative refolding a disulfide bond can form in any of the four repeats. In contrast, peak $HcpB_{234}$ contains a unique species. Its digestion by trypsin produces oxidized (noncyanylated) peptides from the second, third, and fourth repeats and a reduced (cyanylated) peptide from the first repeat (Table 3). Thus, the major intermediate $HcpB_{234}$ has disulfide bonds in the second, third, and fourth repeat and is reduced in the first repeat.

Occurrence of Non-Native Disulfide Bonds during Oxidative Refolding. The analysis of the material represented by the labeled peaks of Figure 7 shows peptides with either free cysteines or correct disulfide bonds. No doubt, the majority of the reduced and unfolded HcpB molecules refolds without the transitory formation of non-native disulfide bonds. Still, traces of non-native protein could be hidden in the small peaks (marked by a star) following the folded protein N and preceding the major intermediate $HcpB_{234}$. The two small peaks contain material of the same mass as native HcpB and $HcpB_{234}$, respectively, but the analysis of the tryptic peptides failed because of lack of sufficient material. While we cannot strictly exclude the possibility that these peaks contain material with non-native disulfide bonds, wrong disulfide linkage would destroy the repeat nature of the protein and should lead to a more different elution behavior on RP-

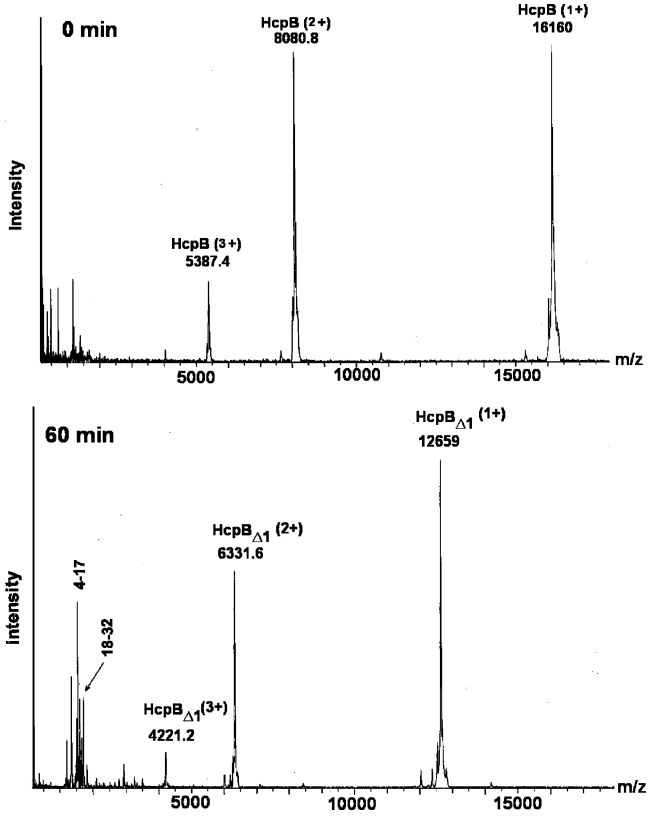

FIGURE 8: Proteolysis of native HcpB with thermolysine. Top panel: ESI-MS spectrum before proteolysis. The monoisotopic mass of the singly charged protein is 16 160. Bottom panel: ESI-MS spectrum after 1 h proteolysis with thermolysine. The monoisotopic mass of the singly charged fragment is 12 659 corresponding to the sequence 33−144 (HcpB$_{\Delta}$1). The identity of HcpB$_{\Delta}$1 was confirmed by automated Edman degradation, which yielded the N-terminal sequence LVSNSQ. Within the cluster of peaks with m/z < 2000, two peptides could be assigned to the first repeat, as indicated.

HPLC. Therefore, it seems unlikely to us that these minor peaks indicate folding through a non-native disulfide pattern.

The Nature of the Main Folding Intermediate HcpB$_{234}$. The main folding intermediate is stable for days when kept in argon-saturated standard buffer at pH 7 and 25 °C. This remarkable property permitted us to study its nature in more detail. Figure 5 shows the CD spectrum of HcpB$_{234}$. The spectrum is positioned about three-quarters between the spectra of fully reduced and native HcpB, which would agree with three folded and one unfolded repeat. By a fortuitous observation, we were able to compare intermediate HcpB$_{234}$ with a derivative of HcpB truncated by the first repeat. Incubation of native HcpB with thermolysine at a protein-to-enzyme ratio of 100:1 produces one major cleavage product corresponding to the sequence 33−144 (Figure 8). Cleavage after Ser-32 occurs in an exposed position near the C-terminal end of helix 1B of the first repeat (Figure 1). The CD spectrum of HcpB$_{\Delta}$1 (Figure 5) indicates that the three repeats of the truncated derivative are folded as in the native protein. This follows from the near to identical spectra of HcpB$_{\Delta}$1 and HcpB when the spectra are expressed as ellipticity per mole of residue (MRE).

The First Repeat Contributes Most to the Stability of HcpB. Figure 9 compares the urea unfolding curve of native HcpB with the unfolding curves of the major intermediate HcpB$_{234}$ and the truncated intermediate HcpB$_{\Delta}$1. In terms of the

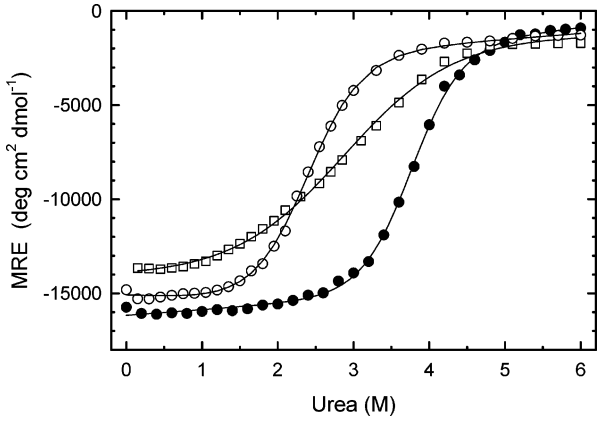

FIGURE 9: Urea unfolding curves of native HcpB, major intermediate HcpB$_{234}$, and truncated derivative HcpB$_{\Delta}$1. Solid lines are best fits for two-state unfolding for native HcpB (●), $\Delta G_U^W = 27.3$ kJ mol^{-1}, $m = 7.3$ kJ mol^{-1} M^{-1}; major intermediate HcpB$_{234}$ (□), $\Delta G_U^W = 11.3$ kJ mol^{-1}, $m = 3.8$ kJ mol^{-1} M^{-1}; and truncated HcpB$_{\Delta}$1 (○), $\Delta G_U^W = 14.0$ kJ mol^{-1}, $m = 6.1$ kJ mol^{-1} M^{-1}. Errors of ΔG_U^W are estimated at ±3 kJ mol^{-1}. Experiments were performed in standard buffer of pH 7 at 25 °C. The curve for native HcpB is the same as the corresponding curve of Figure 4.

midpoint urea concentration of unfolding, HcpB$_{\Delta}$1 and HcpB$_{234}$ are significantly less stable than native HcpB. The free energies of unfolding, ΔG_U^W, can be estimated by the linear extrapolation method (*32*) assuming a two-state unfolding model. The major intermediate HcpB$_{234}$ is about half as stable as native HcpB: $\Delta G_U^W = 11$ kJ mol^{-1} versus $\Delta G_U^W = 27$ kJ mol^{-1}. The values of ΔG_U^W of HcpB$_{234}$ and HcpB$_{\Delta}$1 are very similar, 11 kJ mol^{-1} and 14 kJ mol^{-1}, respectively. This again supports a structure of HcpB$_{234}$ in which the first repeat is unfolded and the remaining three repeats are folded.

Taken together, we conclude that (i) the rate-limiting folding of the first repeat contributes very strongly to the overall stability of native HcpB and that (ii) the folding of the first repeat is strongly coupled to cysteine oxidation. Put differently, it is not the folding per se of the first repeat but the formation of the disulfide bridge that completes folding and contributes strongly to the stability of the native protein. Incidentally, the disulfide bond of the first repeat is fully buried in the three-dimensional structure of HcpB (not shown), and this could make its formation rate-limiting.

But why should the first repeat contribute almost as much to stability as the repeats two, three, and four together? There is a peculiarity to HcpB. Most Hcps have an odd number of helices with the first N-terminal helix acting as a capping structure to protect the hydrophobic core of the protein from the solvent. This is not so in HcpB. Here, the first repeat by itself seems to act as a capping motif. Protecting the core of the molecule from the aqueous environment could explain the high stability gain from folding of the first repeat.

There is another irregularity to the N-terminal first repeat. The geometry of the contact between the first and second repeats differs significantly from the other inter-repeat contacts, as shown in Figure 10. In the figure, interactions between helix B of one repeat and helix A of the following repeat (indicated as helices A* in Figure 10) are compared. Interactions between the second and third repeats and between the third and fourth repeats are super-imposable. The corresponding interactions between helix B of the first

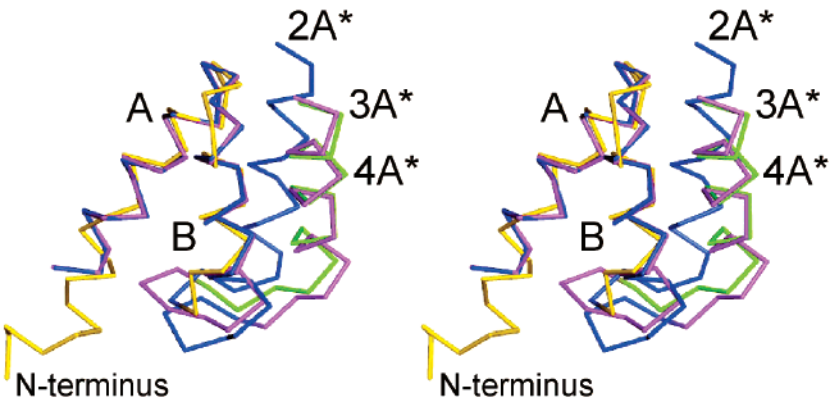

FIGURE 10: Superposition of helices A, B, and A* of HcpB, where A* is helix A of the next repeat. Note that interaction of helix 1B of the first repeat (indicated as yellow helix B) with helix 2A of the second repeat (indicated as blue helix 2A*) differs from the other inter-repeat interactions. When comparing single repeats, helices A and B are super-imposable. The superposition was calculated based on the coordinates of helices A and B of each repeat and neglecting the coordinates of helix A* of the subsequent repeat. Color code is as in panel a of Figure 1.

repeat and helix A* of the second repeat differ significantly. An altered geometry between the first two repeats may have to do with the capping function of the first repeat and may also explain the easy formation of the truncated derivative $HcpB_{\Delta}1$ by limited proteolysis.

GENERAL DISCUSSION

The cysteine-rich repeat proteins from *H. pylori* are characterized by regularly spaced disulfide bonds, one disulfide bond linking the two α-helices of each repeat. The four disulfide bonds of HcpB contribute very significantly to the stability as follows from a comparison of the urea unfolding curves. Unfolding of HcpB with intact disulfide bonds is a reasonably cooperative process. Reduction of the four disulfide bonds removes about half of the CD signature of the α-helix structure of native HcpB and makes refolding noncooperative. Hence, the reduced protein has a poorly ordered structure and retains only about half of the secondary structure of native HcpB. Unfortunately, the overall energy contribution of the four disulfide bonds could not be quantified from the available data because unfolding of reduced HcpB is noncooperative.

The thermodynamic data suggest that thermal unfolding of HcpB with intact disulfide bonds is not an all-or-none process. In an initial phase, the protein gradually accumulates thermal energy leading to partial disruption of packing interactions and increased flexibility. The main, quasi two-state unfolding transition is cooperative, yet it appears that in the transition zone the protein passes through a relatively compact state with grossly disrupted helical structure. As expected, the disulfide links prevent complete exposure of the denatured state to the solvent. The low specific unfolding enthalpy, entropy, and heat capacity of the main unfolding event describe the transition from a suboptimally packed species to an ensemble of not yet fully unfolded polypeptide chains. However, the enthalpic and entropic contributions effectively counterbalance and render HcpB as stable as many other proteins of this size (*26*).

The regular disulfide pattern leads to a rather simple mechanism of disulfide formation. First, folding intermediates appear with a correct disulfide bond in any of the four repeats. Thereafter, the unique three-disulfide intermediate $HcpB_{234}$ builds up and is oxidized to the native protein in a rate-limiting reaction. Intermediate $HcpB_{234}$ has an unstructured N-terminal repeat whose folding is initiated by disulfide formation and contributes about half of the overall free energy of native HcpB. This can be rationalized by an atypical structure and a capping function of the N-terminal repeat and by its disulfide bond being completely buried in the folded molecule. Viewed differently, the formation of the stable folding intermediate $HcpB_{234}$ may be an inherent consequence of early structure formation within three of the four repeats, in agreement with a partial repeat structure of the reduced protein and with the nativelike structure of truncated $HcpB_{\Delta}1$.

As oxidative refolding of HcpB in the test tube follows a direct pathway without wrong disulfide intermediates, the same may apply in the cell. Two enzyme systems are necessary for oxidative folding of disulfide-containing proteins in *E. coli* (*19*). The DsbA/DsbB system oxidizes cysteines as they appear in the periplasm and may produce non-native disulfides. These are reshuffled by the DsbC/DsbD system, which reduces disulfide bonds for reoxidation by DsbA/DsbB. The DsbC/DsbD system is not necessary if disulfide bonds are sequential (*33*). We could confirm that the consecutive array of disulfide bonds of HcpB is formed without reshuffling of wrong disulfides in the periplasm of *E. coli* ((*34*) and V. Sathya Devi, unpublished experiments). Formation of HcpB was demonstrated in Western blots of protein extracts from *E. coli* mutants lacking the DsbC/DsbD system but not in mutants lacking the cysteine oxidizing DsbA/DsbB system. Thus, the simple pattern of disulfide formation we have observed in the test tube also seems to hold in the cell.

REFERENCES

1. Main, E. R., Jackson, S. E., and Regan, L. (2003) The folding and design of repeat proteins: reaching a consensus, *Curr. Opin. Struct. Biol. 13*, 482−489.
2. Main, E. R. G., Stott, K., Jackson, S. E., and Regan, L. (2005) Local and long-range stability in tandemly arrayed tetratricopeptide repeats, *Proc. Natl. Acad. Sci. U.S.A. 102*, 5721−5726.
3. Groves, M. R., and Barford, D. (1999) Topological characteristics of helical repeat proteins, *Curr. Opin. Struct. Biol. 9*, 383−389.
4. Kobe, B., and Kajava, A. V. (2000) When protein folding is simplified to protein coiling: the continuum of solenoid protein structures, *Trends Biochem. Sci. 25*, 509−515.

5. Andrade, M. A., Perez-Iratxeta, C., and Ponting, C. P. (2001) Protein repeats: structures, functions, and evolution, *J. Struct. Biol. 134*, 117−131.
6. Amstutz, P., Binz, H. K., Parizek, P., Stumpp, M. T., Kohl, A., Grutter, M. G., Forrer, P., and Pluckthun, A. (2005) Intracellular kinase inhibitors selected from combinatorial libraries of designed ankyrin repeat proteins, *J. Biol. Chem. 280*, 24715−24722.
7. Binz, H. K., Amstutz, P., Kohl, A., Stumpp, M. T., Briand, C., Forrer, P., Grutter, M. G., and Pluckthun, A. (2004) High-affinity binders selected from designed ankyrin repeat protein libraries, *J. Mol. Biol. 22*, 575−582.
8. Mello, C. C., and Barrick, D. (2004) An experimentally determined protein folding energy landscape, *Proc. Natl. Acad. Sci. U.S.A. 101*, 14102−14107.
9. Tang, K. S., Fersht, A. R., and Itzhaki, L. S. (2003) Sequential unfolding of ankyrin repeats in tumor suppressor p16, *Structure 11*, 67−73.
10. Devi, V. S., Binz, K. H., Stumpp, M. T., Pluckthun, A., Bosshard, H. R., and Jelesarov, I. (2004) Folding of a designed simple ankyrin repeat protein, *Protein Sci. 13*, 2864−2870.
11. Cao, P., McClain, M. S., Forsyth, M. H., and Cover, T. L. (1998) Extracellular release of antigenic proteins by *Helicobacter pylori*, *Infect. Immun. 66*, 2984−2986.
12. Mittl, P. R. E., Luthy, L., Hunziker, P., and Grutter, M. G. (2000) The cysteine-rich protein A from *Helicobacter pylori* is a beta-lactamase, *J. Biol. Chem. 275*, 17693−17699.
13. Graham, D. Y., and Yamaoka, Y. (1998) *H. pylori* and cagA: relationships with gastric cancer, duodenal ulcer, and reflux esophagitis and its complications, *Helicobacter 3*, 145−151.
14. McGee, D. J., and Mobley, H. L. (1999) Mechanisms of *Helicobacter pylori* infection: bacterial factors, *Curr. Top. Microbiol. Immunol. 241*, 155−180.
15. Krishnamurthy, P., Parlow, M. H., Schneider, J., Burroughs, S., Wickland, C., Vakil, M. B., Dunn, B. E., and Phadnis, S. H. (1999) Identification of a novel penicillin-binding protein from *Helicobacter pylori*, *J. Bacteriol. 181*, 5107−5110.
16. Deml, L., Aigner, M., Decker, J., Eckhardt, A., Schutz, C., Mittl, P. R. E., Barabas, S., Denk, S., Knoll, G., Lehn, N., and Schneider-Brachert, W. (2005) Characterization of *Helicobacter pylori* cysteine-rich protein A as a T-helper cell type-1 polarizing agent, *Infect. Immun. 73*, 4732−4742.
17. Li, N., Chibber, B. A. K., Castellino, F. J., and Duman, J. G. (1998) Mapping of disulfide bridges in antifreeze proteins from overwintering larvae of the beetle *Dendroides canadensis*, *Biochemistry 37*, 6343−6350.
18. Luthy, L., Grutter, M. G., and Mittl, P. R. E. (2002) The crystal structure of *Helicobacter pylori* cysteine-rich protein B reveals a novel fold for a penicillin-binding protein, *J. Biol. Chem. 277*, 10187−10193.
19. Collet, J. F., and Bardwell, J. C. (2002) Oxidative protein folding in bacteria, *Mol. Microbiol. 44*, 1−8.
20. Sevier, C. S., and Kaiser, C. A. (2002) Formation and transfer of disulphide bonds in living cells, *Nat. Rev. Mol. Cell Biol. 3*, 836−347.
21. Plotnikov, V. V., Brandts, J. M., Lin, L. N., and Brandts, J. F. (1997) A new ultrasensitive scanning calorimeter, *Anal. Biochem. 250*, 237−244.
22. Makhatadze, G. I., Lopez, M. M., and Privalov, P. L. (1997) Heat capacities of protein functional groups, *Biophys. Chem. 64*, 93−101.
23. Milev, S., Gorfe, A. A., Karshikoff, A., Clubb, R. T., Bosshard, H. R., and Jelesarov, I. (2003) Energetics of sequence-specific protein−DNA association: conformational stability of the DNA binding domain of integrase Tn916 and its cognate DNA duplex, *Biochemistry 42*, 3492−3502.
24. Gomez, J., Hilser, V. J., Xie, D., and Freire, E. (1995) The heat capacity of proteins, *Proteins 22*, 404−412.
25. Makhatadze, G. I. (1998) Heat capacities of amino acids, peptides and proteins, *Biophys. Chem. 71*, 133−156.
26. Robertson, A. D., and Murphy, K. P. (1997) Protein structure and the energetics of protein stability, *Chem. Rev. 97*, 1251−1267.
27. Cheng, Y. H., Yang, J. T., and Chau, K. H. (1974) Determination of the helix and β form of proteins in aqueous solution by circular dichroism, *Biochemistry 13*, 3350−3359.
28. Ferreon, A. C. M., and Bolen, D. W. (2004) Sizes of native and denatured species as a function of denaturant concentration, pH and temperature, *Biophys. J. 86*, 618a−619a.
29. Anfinsen, C. B., Haber, E., Sela, M., and White, F. H. (1961) The kinetics of formation of native ribonuclease during oxidation of the reduced polypeptide chain, *Proc. Natl. Acad. Sci. U.S.A. 47*, 1309−1314.
30. Ruoppolo, M., Pucci, P., and Marino, G. (2005) Folding and disulfide formation, in *Protein Folding Handbook* (Buchner, J., and Kiefhaber, T., Eds.) pp 946−964, Wiley-VHC, Weinheim, Germany.
31. Wu, J., Yang, Y., and Watson, J. T. (1998) Trapping of intermediates during the refolding of recombinant human epidermal growth factor (hEGF) by cyanylation, and subsequent structural elucidation by mass spectrometry, *Protein Sci. 7*, 1017−1028.
32. Pace, C. N. (1986) Determination and analysis of urea and guanidine hydrochloride denaturation curves, *Methods Enzymol. 131*, 266−280.
33. Berkmen, M., Boyd, D., and Beckwith, J. (2005) The nonconsecutive disulfide bond of *Escherichia coli* Phytase (AppA) renders it dependent on the protein-disulfide isomerase, DsbC, *J. Biol. Chem. 280*, 11387−11394.
34. Devi, V. S. (2005) Folding of repeat proteins: Designed ankyrin repeat and cysteine-rich repeat protein from *Helicobacter pylori*, Ph.D. Thesis, pp 54−68, University of Zurich, Zurich, Switzerland.

BI052352U